EXPERIMENTAL INVESTIGATION OF BOILING HEAT CONVECTION IN A FRACTURE

A REPORT SUBMITTED TO THE DEPARTMENT OF PETROLEUM ENGINEERING IN PARTIAL FULFILLMENT OF THE REQUIREMENTS FOR THE DEGREE OF MASTER OF SCIENCE

by

Robert J. DuTeaux

December 14, 1998

ABSTRACT

This report focuses on the coupling between heat conduction and heat convection with boiling flow in a rock fracture. An experimental investigation attemped to analyze and quantify this coupling, which can be called a boiling convection coefficient. This coefficient is the proportionality factor between the heat flux to a fracture surface and the temperature of the rock near a fracture as water boils on that surface. Two types of experimental investigations, one transient experiment with boiling on a nonporous glass surface, and one steady state experiment with boiling on the surface of a rock from a geothermal reservoir, were conducted. On nonporous surfaces, the heat flux described by a boiling regime is strongly coupled to the flow regime of the fluid flowing along that surface. However, on a porous rock surface the near-surface temperature of the rock is prescribed by thermodynamics and controlled by measurable parameters such as porosity and permeability. The excess temperature associated with boiling appears to be much less coupled to the flow of fluid on that surface. These results encourage the development of a discrete fracture network model for a geothermal reservoir that would use a convection coefficient for coupling conductive heat transport in unfractured rock to the convective heat transport with fluid in fractures. Although more research is needed to construct a model, such a model could be useful for predicting the propagation of a thermal front associated with injection into vapor dominated reservoirs.

ACKNOWLEDGMENTS

This research was supported by DOE contract DE-FG07-95ID13370. The support of Dr. Roland Horne in the pursuit of new approaches to challenging problems and the freedom to pursue unexplored territory is greatly appreciated. I am grateful also to Bill Brigham, Shaun Fitzgerald and Cengiz Satik for their guidance. I was also honored to have the support of M-many friends, Marilou, Michelle, Meiqing, and Martha. Thank you.

TABLE OF CONTENTS

1 INTRODUCTION

1.1 Dimensional Scales

Water injected into a geothermal reservoir travels through the reservoir on a time scale established by the mean arrival time of a tracer at a production well and on a length scale defined by the separation distance between wells. Modeling the time and distance scales of fluid and thermal energy transport in fractured reservoirs, however, has been difficult because pressure and temperature changes occur on very different dimensional scales in flowing fractures and in unfractured rock. For example, while tracers (and therefore heat) can be transported by fluid convection through fractures tens or even hundreds of meters in only a few hours (Grant 1982, Horne 1982), heat flow in low permeability unfractured rock can require on the order of 30 years to diffuse 30 meters away from a temperature perturbation (Pruess 1990). This is due to the physical properties of rocks in fractured geothermal reservoirs which typically have small thermal conductivities (for example see Walters and Combs 1991), low porosity (for example see Gunderson 1991), and very small intrinsic (unfractured matrix) permeabilities (Reed 1998). This means that the spatial and temporal discretizations employed in a geothermal reservoir simulation designed to model the dimensional scales of fluid and tracer transport in fractures may have significant difficulty resolving the scale of distances associated with diffusion phenomena that occur in unfractured rock. The characteristic time and distance scales of transport models for fractured rock often cannot simultaneously represent phenomena in unfractured rock with desired accuracy. Since reinjection of thermally depleted water is common in the operation of geothermal reservoirs around the world, the ability to model the physical processes associated with reinjection has been an important aspect of reservoir engineering.

1.2 Development of a Discrete Fracture Network Model

One modeling approach that has been applied successfully to the simulation of chemical transport in fractured reservoirs is to formulate a fractured network

model. Since chemical diffusion induced by a concentration gradient is analogous to heat diffusion driven by a temperature gradient, it seems appropriate to investigate the possibility of constructing a fracture network model for a geothermal reservoir. Such a model simulates the different transport mechanisms in fractures and unfractured matrix separately, and then couples the two models together by describing the boundary condition between them. Therefore fractures and matrix are modeled as discrete entities, each with their own transport mechanisms and characteristic dimensional scales. In order to construct such a model, a relationship that describes the coupling between transport in fractures and the unfractured rock matrix must be developed. For example, with chemical transport in fractured reservoirs the coupling can be described by adsorption isotherms. This report, however, describes the research that has been conducted to analyze and quantify the coupling between heat conduction in rock and heat advection with fluid in a fracture. This research has focused on the relationship between the boiling temperature near a fracture surface and the heat flux to that surface. The proportionality factor between these two quantities will hereafter be called a boiling convection coefficient.

1.3 Two Areas of Research Required

There are two main research efforts required for developing a fractured network geothermal model with boiling and multiphase flow: 1.) A complete mathematical description of two phase flow (and all possible flow regimes) in a rock fracture; and 2.) A quantification of boiling/condensing convection coefficients to quantify the heat exchange between the rock matrix and flowing fractures. Literature on boiling and condensation with multiphase flow in heat exchangers provides a basis for understanding how a fractured network model could be constructed, however, flow and boiling in rock fractures is influenced by the porous nature of those surfaces, and further research needs to be conducted in order to investigate these differences. While the mathematical description of multiphase flow in fractures may be the most difficult aspect of developing a discrete fracture model, this report concentrates primarily upon analyzing and quantifying the

boiling convection coefficient, with a minor analysis of multiphase flow and flow regimes inspired by visual observations made during experiments.

2 BACKGROUND ON DIMENSIONAL SCALES AND MODELING

2.1 Thermal Diffusivity

The characteristic dimensional scales for thermal energy transport in unfractured rock depend upon the intrinsic permeability and thermal diffusivity of the rock. For the heat transport in very low permeability rock, the thermal diffusivity of the rock determines how far a temperature perturbation travels through the unfractured reservoir in a given amount of time. Thermal diffusivity (α) is the ratio thermal conductivity / volumetric heat capacity of a rock; $\alpha = k / \rho C_p$, where ρ denotes density and C_p denotes heat capacity. Thermal diffusivity is a property that describes and couples the characteristic time and length dimensional scales for conductive heat diffusion. Many rocks, including geothermal rocks, have thermal diffusivities on the order of 1.0 E -6 m^2/s. The Fourier number (Fo), dimensionless time, is the ratio of the heat conduction rate to the rate of thermal energy storage in a solid; $Fo = (\alpha t) / L^2$, where t denotes time and L denotes length or distance. Setting this ratio equal to one and rearranging terms reveals the expressions for characteristic length (L_c), or characteristic time, (t_c).

$L_c = \sqrt{(\alpha t)}$ or similarly, $t_c = L^2 / \alpha$ α = thermal diffusivity (2.1.1)

Plugging the value of 1.0 E -6 m^2/s for the thermal diffusivity of rock and the time of 30 years into Equation 2.1.1 results in a characteristic length of about 30 meters.

Furthermore, the diffusion of hydraulic pressure and dissolved chemical species into unfractured rock are analogous to the diffusion of heat into very low permeability rock, and often operate on similar dimensional scales.

In unfractured rocks the intrinsic hydraulic diffusivity determines the distance a pressure perturbation travels in a given time. Since temperature gradients drive heat conduction, and pressure gradients drive fluid flow, the thermal and

hydraulic diffusivities of reservoir rocks are properties that regulate the dimensional scales for the transport of heat and fluid. Since pressure changes propagate quickly through fractures but slowly through a low permeability matrix, nonequilibrium conditions of temperature and pressure in fractured rock may persist during injection and exploitation of geothermal reservoirs. In fractured reservoirs, the fluid velocity through the fractures can be many orders of magnitude greater than in the unfractured rock, and because heat is convected by the fluid in fractures, both heat and fluid travel across reservoir distances much faster than they do in unfractured matrix rock.

2.2 Efficiency of Heat Mining - Dimensional Scales

One reason for injecting thermally depleted water is to extract more of the total heat energy of a reservoir, which is contained largely in the heat capacity of the reservoir rock, rather than the *in-situ* fluid. Therefore, a consideration for the efficiency of producing additional energy can be made that illustrates the dimensional scales of thermal energy transport in fractured reservoirs. For example, if the thermal time constant (characteristic time) required for heat to diffuse from the midpoint between flowing fractures is much less than the mean tracer residence time in an adjacent fracture, the injected fluid will extract a large fraction of the heat available in the rock. Analysis shows that when flowing fractures are spaced on the order of a few meters or less, the assumption of thermodynamic equilibrium between the rock and the fluid can be justified if the fluid velocity is not exceptionally great. In this case, a relatively uniform thermal front will propagate spatially outward from the injection well. If, however, the time required for thermal diffusion between fractures is much greater than the fluid residence time in adjacent fractures, cold fluid will “finger” down the fracture surfaces toward a production well leaving great quantities of energy in place. The rate of propagation of a thermal front outward from an injection well, and the fraction of total reservoir energy produced are therefore strongly dependent upon the contrast between the velocity of flow in fractures and the rate of thermal energy transport in the unfractured reservoir matrix.

2.3 Simple Analytical and Numerical Models

Several significant publications develop analytic and numerical solutions for fluid flow and heat transfer fractured rock. (for early examples see Bodvarsson 1974 and 1982, Gringarten 1975, Kuo 1975 and 1976, Weeler 1969). A relatively simple solution for one-dimensional conduction from an infinite medium normal to single-phase flow in a fracture is given by Carslaw and Jaeger (1959) in their text on heat conduction. These studies illuminate the important relationships between flow rates, thermal time constants, and characteristic dimensions, but concern single-phase flow in only simplistic geometries. While a thorough understanding of dimensional scales can be derived from these works, such models are generally not a sufficient basis for making many of the operating decisions that have to be made by reservoir engineers, and so more sophisticated numerical models have been developed.

2.4 Porous Continuum Models

Borrowing heavily from petroleum and groundwater simulation technology, the method that has been most widely applied to commercial geothermal reservoirs is a porous continuum approach, where the hydraulic properties of the fractures and matrix are combined with the concept of a representative elemental volume (REV) and simulated on a reservoir scale.

The idea of a REV is fundamental to the derivation of the continuity of mass, momentum, and energy equations in a continuum model. This volume defines a characteristic dimensional scale for the discretization of a simulation model. Valid volume elements in a simulation must be as big or larger than a REV. On the REV scale, reservoir quantities are considered uniformly distributed. That is, any larger volume would have the same properties, but smaller volumes would not necessarily represent reservoir properties on a simulation scale. Thus, the standard formulation of a continuum assumes homogeneous porosity, permeability, phase saturations, and temperature within a REV. Thus, thermodynamic equilibrium within each volume element is assumed. The unavoidable problem in modeling a fractured geothermal reservoir as a

continuum is that the REV must be larger than the spacing of major permeable fractures in order to model permeability in a continuum. Since some geothermal reservoirs have large scale fault-controlled permeability (for example see Beowawe Nevada, Faulder 1997), this implies that a REV could be larger than the injection-production well spacing. A continuum formulation, however, is the standard model because the dynamics of fluid flow and phase transition in porous media have a relatively broad foundation of technology, being widely applied in the petroleum industry.

2.5 Dual Porosity Models

Acknowledging the contrast in dimensional scales for fractured reservoirs has thus led to a double porosity (dual continuum) approach for modeling such reservoirs (Warren and Root 1963). This separates the properties of a fractured reservoir into multiple continua. These continua include a connected continuum representing the dimensional extent and properties of fractures, surrounding multiple continua that represent the unfractured blocks of rock matrix. The unfractured matrix continua have porosities, permeabilities, and other properties that contrast with the fractured continuum. Since numerical difficulties arise when steep temperature or pressure gradients develop between adjacent discretized regions, the fractures are not spatially discrete. Rather, adjacent discretized elements have intermediate properties that gradually transition from those of the fractures to those of the matrix. This means that the two-dimensional planar geometry of fractures must be "smeared" into three-dimensional volumes including elements representing fractured continuum, intermediate continua, and matrix continua.

Dual porosity models are the current industrial standard for simulating fractured reservoirs, however, some of the fundamental physical assumptions made for these models continue to require further scientific verification. For example, both capillary continuity and relative permeability in fractures, which have powerful influences in reservoir simulations, remain controversial (compare W. Chen 1987, J. Chen 1991, and Kazemi 1979 1992 to Firoozabadi 1990 and Labastie

1990 on capillary continuity; compare results from Corey 1954, Council 1979, Ambusso 1996, and Fulcher 19?? on relative permeability). In continuum and dual continuum models no physical representation of the actual geometry or hydraulic properties of fractures is made, even though the hydraulic nature of fractures has been shown to differ from porous media (Witherspoon 1980). Instead, hydrologic behavior relies upon Darcy flow in porous media and upon relative permeability curves. Furthermore, these models generally do not include some of the potentially significant couplings between permeability and pore pressure (Boitnott 1990, Ozdogan 1994), thermally-induced rock deformation (Harlow 1972, Tester 1989) or mineral precipitation/dissolution (D'Amore 1983, Robinson 1982), and do not account for the documented adsorption of injected liquid in vapor-dominated systems (Hornbrook 1994).

With these considerations, and yet a great respect for the sophistication and utility of modern continuum models, this research examines the possibility of developing a more physically based model of the thermal and hydraulic behavior of a discrete fracture.

3 BACKGROUND - BOILING CURVE, BOILING AND FLOW REGIMES

3.1 Nucleation and Boiling

Excess temperature, (ΔT_e), defined as $\Delta T_e = T_{surface} - T_{saturation}$, is required for the nucleation of bubbles in a boiling process. However, the surface tension of a fluid and the size distribution of small asperities (and their geometry) on a surface influences the ΔT_e required for nucleation. For example, very smooth surfaces require large excess temperatures because the radii of curvature of bubbles begin infinitely small and require very large pressure differences between the vapor and the liquid to expand the bubbles. On rough surfaces, bubbles may expand more easily because they begin in the sharp crevices and expand with larger radii of curvature. In porous media, the size of the pores relates to the thermodynamics of vaporization and the mobilization of vapor (Udell 1982). This suggests that the boiling process begins with physical dynamics that are specific to the fluid and the surface or pore space involved.

Although no rigorous theory exists, it is generally accepted that bubbles departing from a surface promote the mixing of a superheated boundary layer with the bulk fluid, and the bulk fluid displaces the volume previously occupied by the bubble bringing cooler fluid into contact with the surface. Research has demonstrated that the heat flux during nucleate boiling is proportional to the nucleation site density as well as the excess temperature on a surface (Yamagata 1955).

3.2 Boiling Curves

A commonly employed illustration of the proportional relation between surface heat flux and ΔT_e is the boiling curve shown on the left in Figure 3.2.1. On the right side of this figure is a qualitative comparison of boiling curves for a surface with a porous coating, shown by the black curve, and a nonporous surface, shown by the gray curve. This porous boiling curve is illustrated by Kovalev

(1987), in one of only a few publications that investigate boiling on porous surfaces.

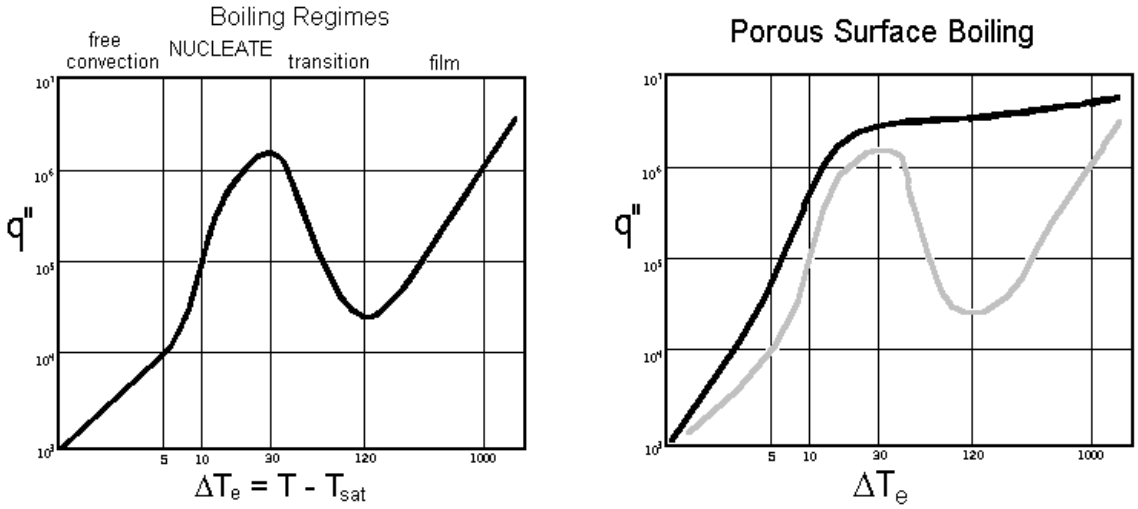

Figure 3.2.1 Boiling Curves for water on nonporous and porous surfaces.

3.3 Boiling Regimes

Boiling regimes describe distinct intervals of the Boiling Curve that are influenced by different liquid/vapor fractions adjacent to the boiling surface. These regimes are strongly coupled to the hydrodynamics of the fluid flowing on a surface because viscous flow along a surface assists the transport of vapor from the boiling surface.

In the region of just a few degrees ΔT_e the fluid is all liquid, and free convection, that is, buoyancy-induced convection, controls the heat exchange and transport from the surface. With the nucleation of bubbles at a slightly higher excess temperature, the curve grows steeper in the nucleate boiling regime. Then, as more vapor is generated at still higher ΔT_e, the heat flux to the surface increases more slowly because the vapor adjacent to the surface has a lower thermal conductivity than the liquid. This region of the curve is labeled “Transition”. For nonporous surfaces at even larger ΔT_e, the heat flux decreases because a larger fraction of the surface remains in contact with less thermally conductive vapor. According to Kovalev (1987), however, surfaces with permeable porous coatings

continue to maintain relatively high heat fluxes. The reasons for this difference are topics for future research.

3.4 The Boiling Convection Coefficient

Heat transfer for internal flow is commonly characterized by the Nusselt number, which can be viewed as a dimensionless convection coefficient and describes the temperature gradient at the surface-fluid contact. The convection coefficient (h) is a factor of proportionality between the heat flux and the temperature difference between a surface and the bulk fluid in accordance with Newton's law of cooling $q" = h(T_{surface} - T_{fluid})$. With boiling, the convection coefficient (h_b) is a function of excess temperature, $h_b = q"/\Delta T_e$, and h_b can be orders of magnitude larger than a single phase convection coefficient.

Fluid properties, as well as rock properties, determine the heat convected with a fluid in a boiling fracture. Surface tension (σ), the latent heat of vaporization (h_{fg}), viscosity (μ), flow velocity (u), fluid conductivity (k_f), the liquid and vapor phase heat capacities ($C_{p,liq/vap}$), and the density difference between the liquid and vapor (ρ_{liq}-ρ_{vap}), gravity g, and length dimension L, are fundamental parameters. In order to reduce the number of functional variables to a minimum these may be grouped into a smaller number of dimensionless groups. The common groups relevant for boiling include the Reynolds number $\rho\, u\, L / \mu$ (Re), the Prandtl number $\mu\, Cp / k_f$ (Pr), the Jakob number $C_p\, \Delta T_e / h_{fg}$ (Ja), and the Bond number $g\, (\rho_{liq}-\rho_{vap}) / \sigma$ (Bo). The Nusselt number $h\, L / k_f$ (Nu), which characterizes the convection coefficient h, is considered a function of these dimensionless parameters (Incropera and DeWitt, 1990), but may also be influence by additional factors in fractured rock.

Empirical studies of boiling quantify either the heat flux at the surface or the convection coefficient as functionally dependent upon these parameters and ΔT_e. One well known example of an empirical relation, valid in the nucleate boiling regime for pool boiling, was developed by Rohsenow in 1952, with q" =

$(\mu_{liq}\ h_{fg})\ [g(\rho_{liq}-\rho_{vap})/\sigma]^{0.5}\ \{C_{p,liq}\ \Delta T_e\ /\ (C_{s,f}\ h_{fg}\ Pr^n)\}^3$, where $C_{s,f}$ and n are characteristic of the surface and fluid to be determined by experimental data. Many similar empirical correlations have been developed in other researchers for various boiling regimes (Lung 1977, and Carey 1992).

Such correlations that quantify a boiling convection coefficient have been based upon empirical studies of multiphase heat exchangers. Many of these relations were developed with either unconfined surfaces, or tubes with horizontal and vertical orientations in heat exchangers for specific flow regimes. They lack the potentially important considerations for flow in porous rock fractures. Clearly, further experimental work with geothermal rocks and fluids will be required to establish a useful empirical relationship between excess temperature and the heat flux to fracture surfaces with boiling flow.

3.5 Flow Regimes

With an understanding of boiling regimes it is easy to understand how the fluid dynamics can affect the convection of heat away from boiling surfaces. The term “flow regime” describes the mechanics of fluid motion in an interval that is distinct from the fluid dynamics at other locations that have different liquid/vapor fractions. Observations have shown that flow regimes influence the heat flux to the boundary of the flow, and the heat flux affects the mechanics of the fluid motion by generating vapor at the margins of flow. Figure 3.5.1 helps to describe the relations between boiling and flow regimes.

Limited analogies to flow in tubes and channels were considered in the developing of Figure 3.5.1, and similar figures can be found in texts on vaporization and condensation in heat exchangers. The effects of porosity, roughness, variable fracture aperture, and the permeable nature of rock surfaces have been neglected in this simple illustration, however, the figure can be useful for a general description of injection into a horizontal fracture. Near the injection location the liquid is subcooled, and heat from the matrix begins a boiling process that proceeds from bubbly flow, to slug flow where bubbles coalesce,

into annular and mist flow until the moving fluid becomes completely vaporized. The boiling regimes in this illustration are divided into nucleate boiling and film evaporation.

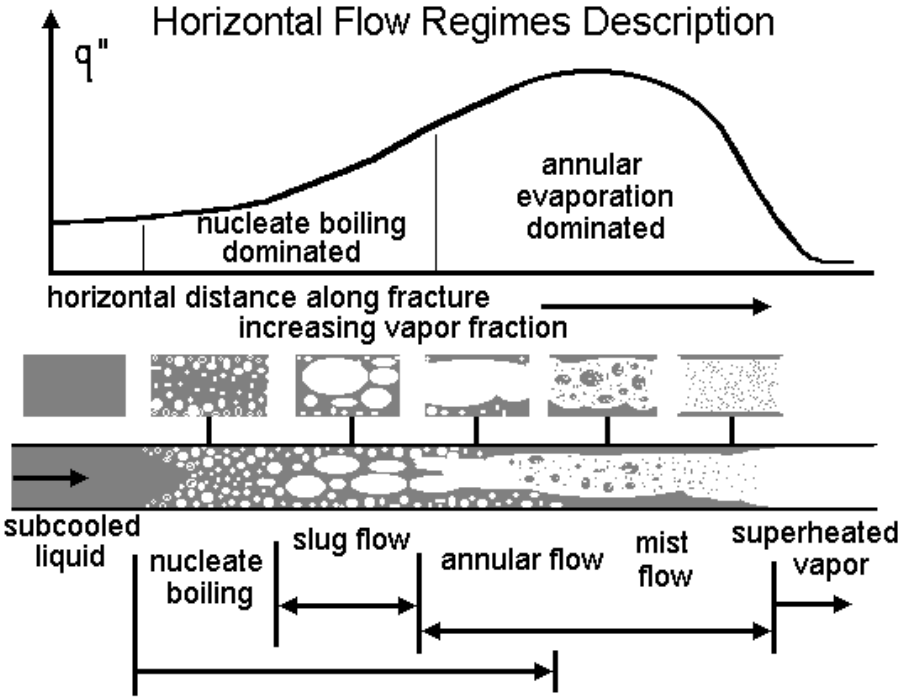

Figure 3.5.1: A qualitative description of boiling and flow regimes.

In Figure 3.5.1, nucleate boiling begins at the margins of the flow and generates bubbles that migrate into the main channel of flow. This occurs at relatively low quality, that is, at relatively small vapor fractions in the flow. As quality increases the mean velocity of the flow increases with the decreasing mean density of the fluid. Annular flow, therefore, may occur with exchanges of momentum between the liquid and vapor fluxes and liquid droplets can become entrained in the vapor flow. As further evaporation occurs, annular film evaporation may become the boiling mechanism at relatively higher fractions of vapor in the channel. Annular film evaporation is a mass flux from the liquid to a vapor phase without the nucleation of bubbles across a thin film of liquid at the margin. In the horizontal

orientation shown, the liquid and vapor can segregate due to density differences and the boundary conditions for heat transfer from above and below the fracture can be different.

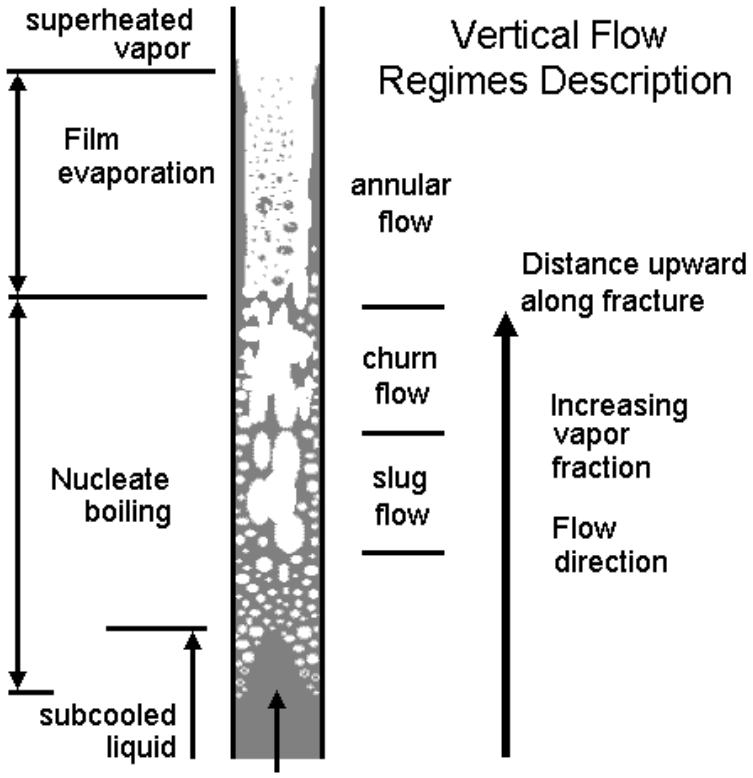

Figure 3.5.2: Boiling and Flow regimes in a vertical fracture.

Figure 3.5.2 is an illustration of flow regimes associated with upward vertical flow. In a vertical fracture the flow regimes may change along the height of the flow path. If subcooled water is injected at the base of a fracture, the flow will transition from free convection to nucleate boiling, then from bubbly flow to slug flow (where bubbles combine), and upward into a region of annular flow where a thin film of liquid evaporates into a predominantly vapor filled aperture. For a constant mass flow rate, the velocity of multiphase flow increases significantly due to the smaller density of the vapor and liquid droplets may be entrained in the vapor flow. Still further upward along the fracture the fluid may become completely superheated.

In this illustration the effect of gravity does not cause a segregation of flow, but it does exert a differential force on the liquid and vapor phases. In vertical flow the buoyancy of the vapor and the interfacial tension between liquid and vapor allow slugs of vapor to push slugs of liquid upward. Under the conditions where these forces were in relative equilibrium, instability occurs and the flow can become chaotic. This is illustrated as the “churn flow” regime.

To summarize, the morphology of a flow regime depends, in part, on how the boiling mechanism at the boundary adds vapor to the flow, and the boiling regime depends, in part, upon how the liquid and vapor fractions of the fluid interact with the margins of the channel. Flow regimes involve the interaction of viscous, capillary, inertial, and buoyancy forces. This interaction of forces depends upon fluid properties and driving potentials, and may be highly influenced by fracture orientation, aperture, and the exchange of momentum between phases. One goal of the experimental research that follows is to investigate the influence of boiling and flow regimes on a boiling convection coefficient, the relationship between rock temperature and the heat flux to a fracture surface.

4 TRANSIENT EXPERIMENT, DESCRIPTION, DATA, AND DISCUSSION

4.1 Description of Apparatus

The experimental apparatus illustrated in Figure 4.1.1 was constructed to measure the heat exchanged between a heated impermeable glass "core" and water flowing upward and boiling in the concentric annulus around the core. The annulus creates an artificial fracture less than one millimeter wide between two large diameter glass tubes with a circumference of about 42 centimeters. The core is a 135 mm (about 5 inches) diameter glass cylinder, closed at the bottom to hold sand that has been heated to a temperature of about 150 ^{o}C. Water flows upward in the annulus on the outside of the glass core, and not in the sand. The sand only provides a medium with a conductivity and heat capacity whose order of magnitude is comparable to rock, in order to develop temperature gradients and heat flow on dimensional scales similar to real rock.

The apparatus is about 0.5 meters (18 inches) tall and has thermocouples attached to the inside and outside of the core. A third concentric cylinder surrounds the artificial fracture to reduce radial heat loss by applying a vacuum. In a typical experiment, water was injected at near atmospheric pressure from the bottom ($z = 0$) at a slow rate, so that (without boiling) it would take a few minutes to reach the top. With boiling, a two-phase zone quickly extends from the base to the top of the apparatus when boiling begins at the base of the fracture.

The glass provides a nonporous impermeable surface, so unfortunately, does not have the porosity, roughness, or a geometry anything like a natural fracture. When preliminary experiments were conducted nucleation sites were sparsely distributed, so a thin film of roughened Teflon was applied to the outside of the cylinder in later experiments to provide better sites for the nucleation of bubbles. This, however, also reduced the wettability of the surface, and these differences must be considered when the data from this apparatus is analyzed.

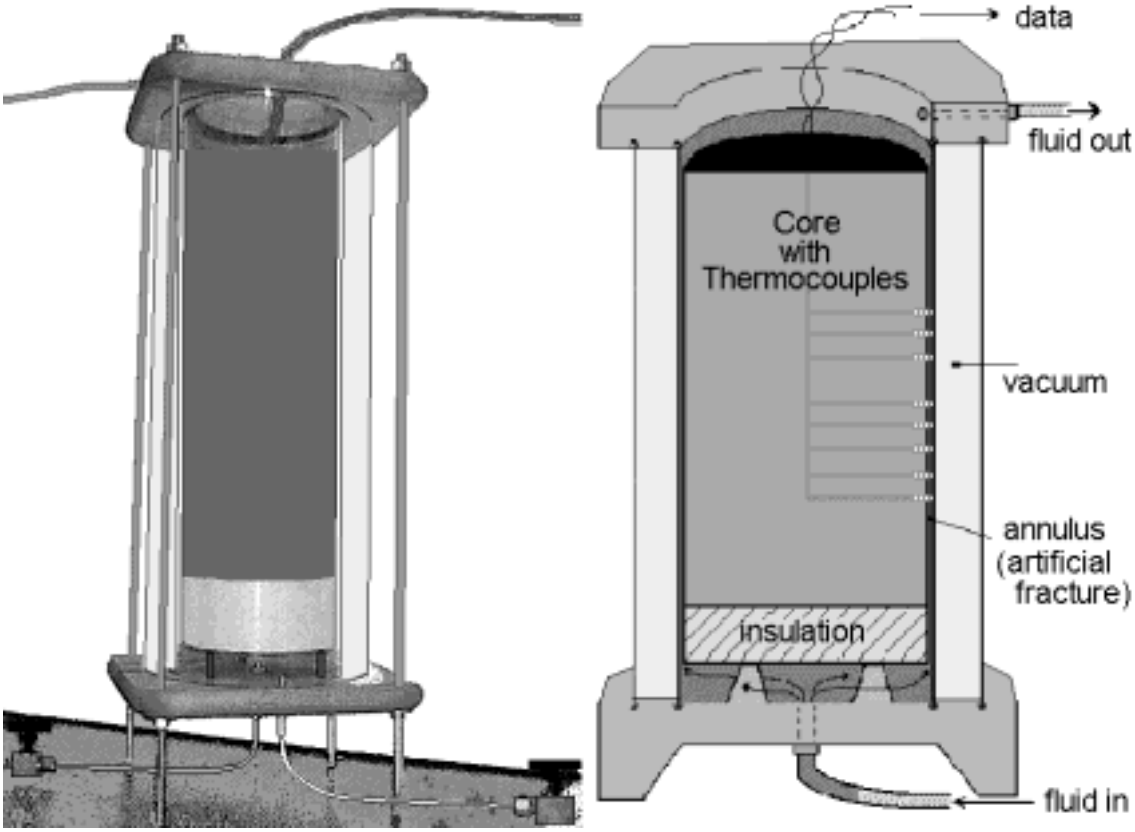

Figure 4.1.1 Nonporous concentric glass cylinders forming an artificial fracture to measure transient temperature gradients and heat flux to a boiling surface.

4.2 Experimental Proceedure

Figure 4.2.1 is a diagram of the system employed to pump liquid water at saturated temperature into the artificial fracture created in the apparatus. The inlet temperature was controlled by a feedback loop to a steam generator, which was later replaced by an immersion heater. A heat exchanger consisting of a container of boiling water on a heater with the injected water passing through a copper coil is labeled saturated liquid water in the diagram.

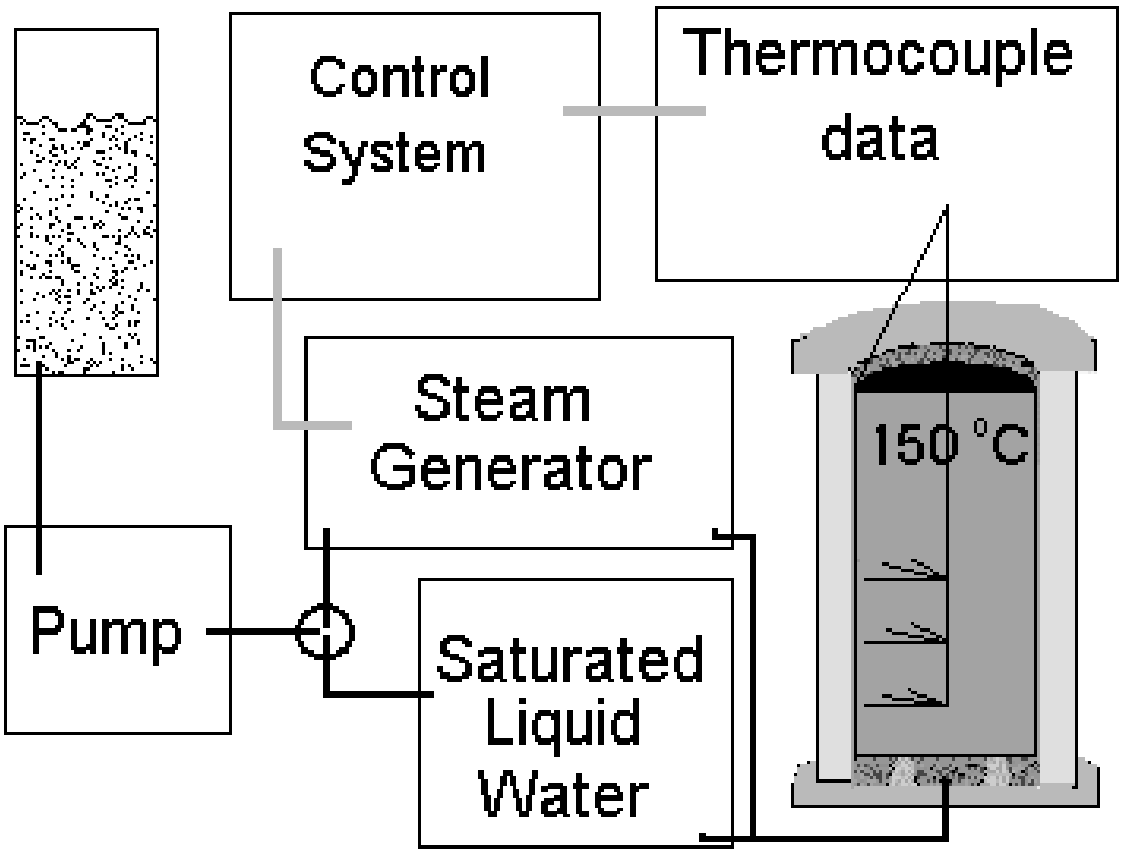

Figure 4.2.1 Experimental System design

In preliminary tests, heat losses due to the thermal capacity of the apparatus caused the temperature of the glass surfaces to decline below the saturation temperature before water reached the heated core. Since only the core of the apparatus was heated, the core holder assembly absorbed enough heat to cool the exterior surface of the core. This problem led to the idea of preheating the assembly with superheated steam using the steam generator or hot air before beginning the experiment. The core was preheated in an oven to a similar temperature in excess of 100 ^{o}C and placed in the assembly. The experiment then began by switching the valve at the pump exit from the steam generator to a supply of saturated liquid water. This saturated liquid then entered the apparatus and flowed up the fracture around the core. The excess temperature of the core caused the water to boil and thermocouples recorded the temperatures in the

fracture, at the inner surface of the core, and radially inward toward the center of the core.

4.3 Experimental Data - Single-Phase Flow

The temperature gradient was recorded and heat fluxes were calculated in single-phase experiments conducted by injecting ice water into the apparatus. Thermocouples were placed at two vertical heights, and heat fluxes were calculated from temperature data, not measured directly. The core was initially at room temperature, with thermocouples placed in the fluid, at the inner surface of the glass, and at one and two centimeters radially farther toward the center. Cold water was pumped through the assembly at 50 ml/min while thermocouple data was recorded. The thermocouples were placed at vertical locations of 21.5 and 26.5 centimeters above the insulation in the bottom of the core. Figure 4.3.1 plots this data, and Figure 4.3.2 shows the transient heat fluxes calculated from the temperature measurements.

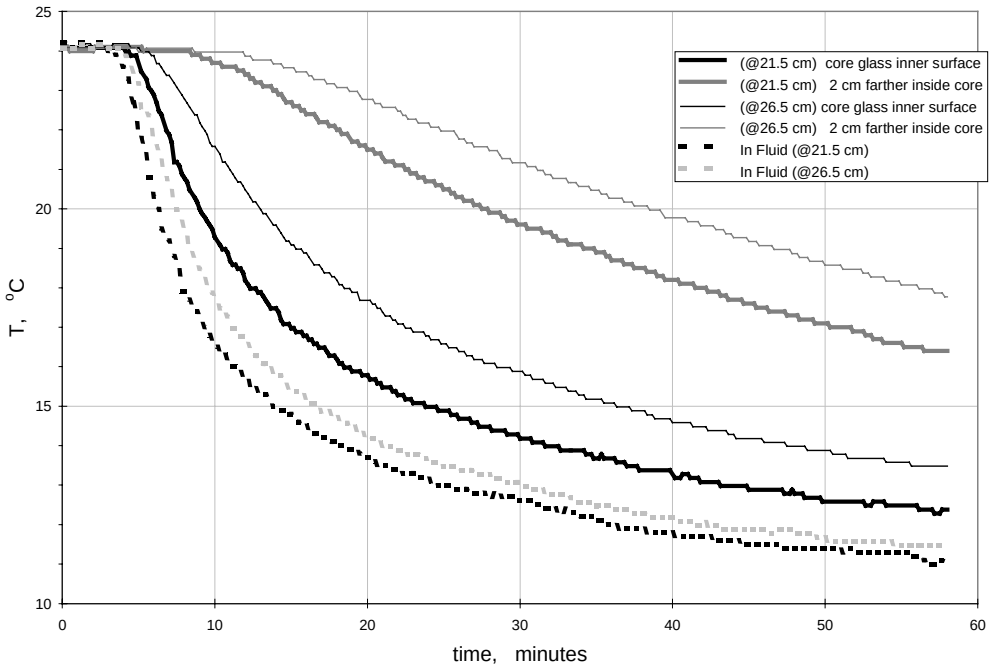

Figure 4.3.1 Radial Transient Temperature measurements with single phase flow.

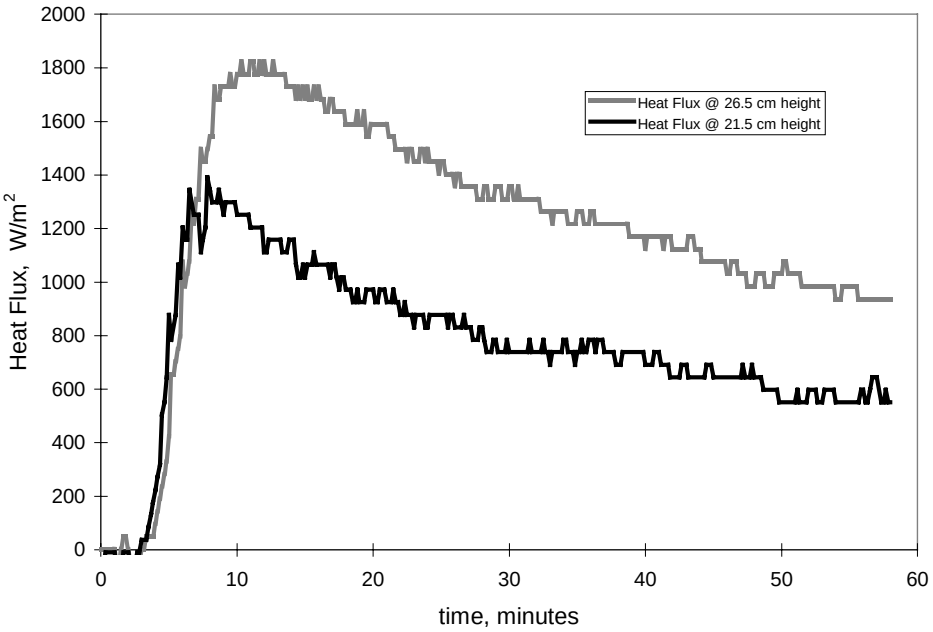

Figure 4.3.2 Transient Heat Flux calculated with single phase flow.

Figures 4.3.1 and 4.3.2 illustrate the propagation of a thermal front past the locations of the thermocouples in the direction of flow. In Figure 4.3.1 the dashed traces are the fluid temperatures at two vertical locations in the fluid and the other traces are temperatures radially inside the core at the same locations. Figure 4.3.2 plots the transient heat fluxes calculated from the temperature gradient across the glass bounding the inner surface of the artificial fracture. This experiment was conducted for comparison to the heat fluxes generated by boiling flow in the same apparatus with a similar temperature difference between the fluid and the core.

4.4 Experimental Data - Boiling Flow

Figure 4.4.1 shows the transient temperatures from a boiling experiment measured with thermocouples placed on the glass surface adjacent to the boiling flow, and on the inner surface (radial inward) of the 3 mm thick glass. This data is similar to the data presented at the 23rd Stanford Workshop on Geothermal

Reservoir Engineering (DuTeaux 1998), but this data is more contemporary and presented in a slightly different manner.

The higher temperatures which begin just above 140 ^{o}C were measured on the inner surface and the lower and more variable temperatures were measured on the outer surface adjacent to the flow. In the initially steep temperature decline at a surface temperature from about 20^{o} above the saturation temperature (100 ^{o}C), to about 10^{o} excess temperature some erratic temperature variations were recorded. These variations are reflected in the heat fluxes plotted in Figure 4.4.2. After an initial period of vigorous boiling, Figure 4.4.1 indicates a relatively linear temperature decline from 10^{o} excess temperature down to the saturation temperature.

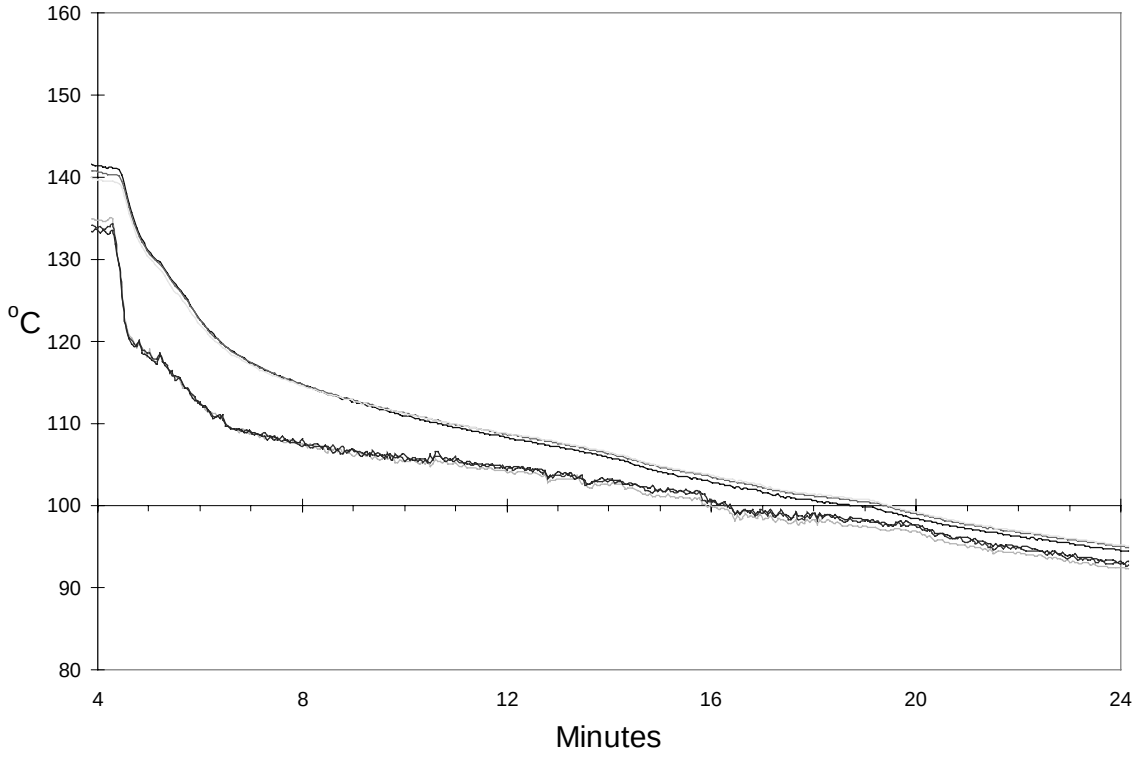

Figure 4.4.1 Temperature data from a transient boiling experiment.

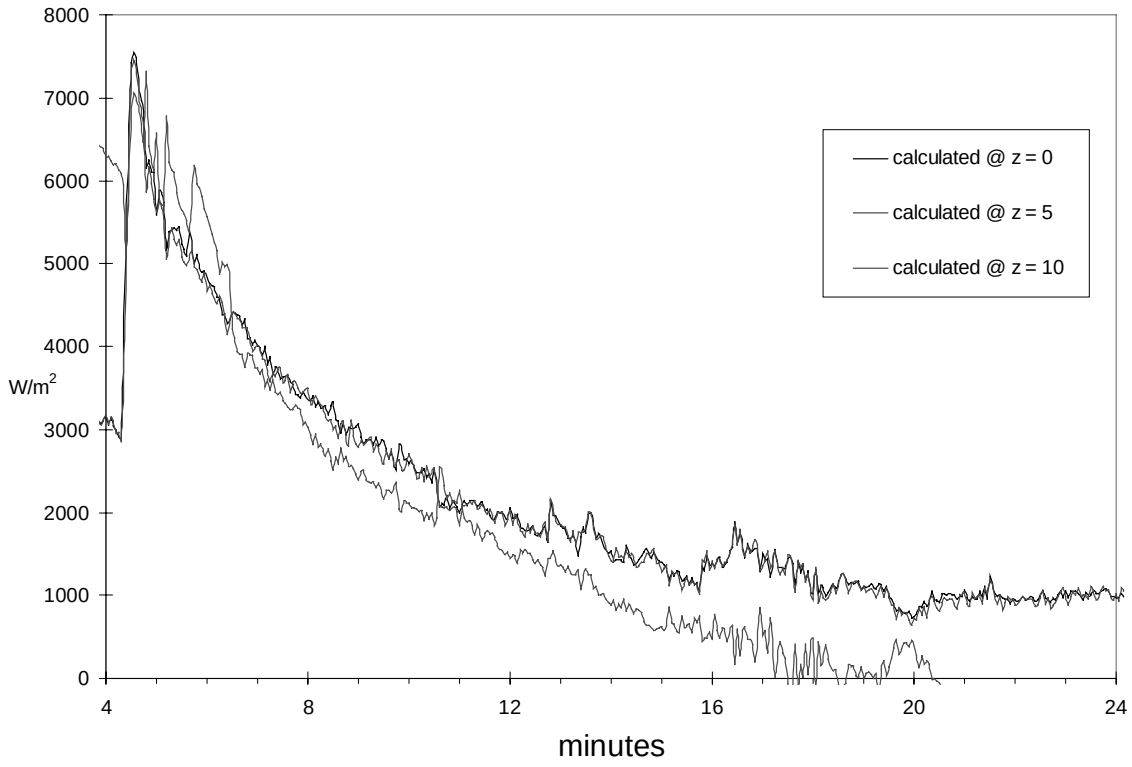

Figure 4.4.2 Heat fluxes calculated from thermocouples separated by 3mm of glass.

The maximum heat flux recorded was a brief transient near 7000 W/m^2 when fluid first entered the fracture and then declined more slowly to about 1000 W/m^2 as the boiling surface declined to the saturation temperature in about 16 minutes.

Figure 4.4.3 is a boiling curve derived from the temperatures and heat fluxes measured during this experiment. Plotting the heat flux versus surface temperature establishes the proportionality between the excess temperature of a surface an the heat flux to that surface. This quantifies a boiling convection coefficient for this apparatus helps to identify the coupled influence of flow and boiling regimes.

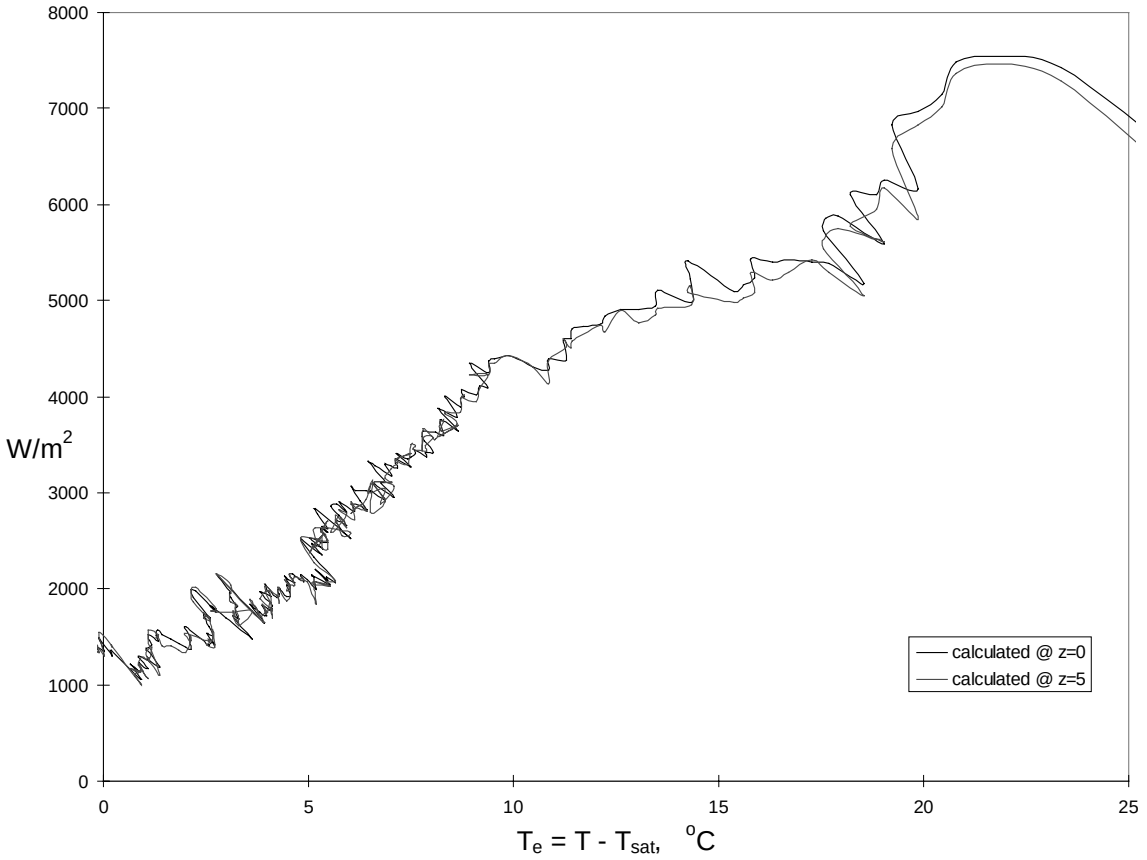

Figure 5.4: A Boiling Curve for a nonporous vertical channel, Heat flux vs excess temperature.

Since the surface temperature declined rapidly while data were recorded once per second, the temperatures closer to saturation temperature have more detail. The cyclic fluctuations in temperature near 20^o excess temperature occurred near the maximum heat flux during the most vigorous boiling when churn flow was observed and recorded on videotape. The video also showed that the flow was actually two-dimensional, with liquid and vapor moving laterally as well as vertically as liquid and vapor phases exchanged momentum. These observations led to the investigation of flow regimes and the coupling with boiling regimes. Generally, different types of flow were visually observed at different times and locations during the experiment. Also, the rate of boiling and the stability or uniformity of flow seems to have been reflected in the temperatures measured.

4.5 Discussion

Comparing the single-phase experiment with the boiling data shows the heat flux associated with boiling, with a similar absolute temperature difference, is more than three times greater than the heat flux to a single-phase flow. The difference in the magnitude of the heat flux at two different locations could be related to nucleation at those locations, but the difference is more likely due to inconsistent calibration of thermocouple outputs. The plots of Figures 4.4.1 and 4.4.2 compared to Figures 4.3.1 and 4.3.2 also illustrate that temperatures and heat fluxes decline faster with boiling because heat is more rapidly depleted from the core. This means that steeper temperature gradients develop near the fracture surface, thus, greater quantities of energy are ultimately transferred to the fluid. Although not unexpected, this result is positive for accessing more of the energy contained in geothermal reservoir rocks.

Closer observation of the temperatures in Figure 4.4.1 allows the delineation of time intervals where temperatures are influenced by flow or boiling regimes. For example, the temperature data can be divided into three intervals, the initial steep decline that lasts about 30 seconds, the moderately steep decline over the next 2 minutes, and the more gradual decline down to saturation temperature over the following 10 minutes. The boiling curve plotted also seems to show three distinguishable intervals that could reflect the coupled boiling and flow effects observed and recorded on videotape.

The cyclic fluctuations in temperature near 20^{o} excess temperature occurred near the maximum heat flux during the most vigorous boiling when churn flow was observed in the fracture. Although the sampling frequency of the data did not allow the resolution of detail in the data, churn flow did cause vapor to push liquid upward in an unstable fashion where gravity caused the liquid to fall back. This also showed the flow was actually two-dimensional, with liquid and vapor moving laterally as well as vertically as phases exchanged momentum. These observations led to investigating the roles of inertial, viscous, buoyancy, and

interfacial forces that influence two-phase flow and boiling in a fracture, and that relative permeability may not be sufficient to describe flow in fractures with large apertures. While pressures were not measured, the exchange of momentum and the potential for segregated flow between phases was apparent. A quantification of these forces and how they affect velocities and pressure drops may be necessary for developing a physical flow model for discrete fractures.

The multiphase extension of Darcy's Law appears only to couple the flow velocities of distinct phases by the capillary pressure between the phases. In fractures, however, capillary forces can be small relative to viscous and buoyancy forces, and phases exchange momentum through the viscous boundary layer between flowing phases. It therefore seems that the phase velocities should be influenced by the exchange of momentum proportionate to the ratio of the surface area to volume of the nonwetting phase, and proportionate to the viscosity of the wetting phase.

These and other questions, especially the validity of measuring a boiling convection coefficient with nonporous surfaces, led to the development of the second experimental apparatus. This apparatus was designed to investigate these competing with steady boiling on the surfaces of real geothermal rock. Data and analysis from this steady state boiling experiment follow in the next section.

5 STEADY STATE BOILING IN A POROUS ROCK FRACTURE

5.1 Boiling on a Porous Rock Surface

Initially, since geothermal rocks often have very low porosities and very small intrinsic permeabilities, nonporous glass surfaces were used to create an artificial fracture. However, over the course of many experiments with glass it became apparent that nucleate boiling and fluid flow across rock surfaces could be considerably different from boiling flow on strictly nonporous surfaces. Also, a method for investigating the interaction of forces with boiling flow in a fracture needed to be researched, therefore, a new apparatus was designed and built. This experiment was designed to quantify the heat flux associated with liquid water flashing to steam in a fracture, similar to the vaporization of injectate in a fractured steam reservoir.

5.2 Experimental Preparations

The apparatus illustrated in Figure 5.1.1 was designed to quantify the heat flux and temperature gradients associated with liquid water flashing to steam in a fracture. Figure 5.1.1 illustrates the assembly in which thermocouples are placed between thin slices of rock beneath the exposed rock face. Beneath the rock is an electrically powered heater, and a glass disk forms the upper boundary of a fracture. The glass disk has a hole at its center for the injection of fluid into the fracture. The rock disks used in this assembly were taken from a graywacke core sample from The Geysers geothermal reservoir in Northern California.

This apparatus was designed to provide a uniform temperature at the base of the rock and a measured heat flux through the rock normal to the flow in the fracture. The apparatus contains three thin rock disks that were prepared with a surface grinder to achieve flat well-mated surfaces. Thermocouples were placed on the aluminum heater box, and at each interface between rock disks. The outer edge of the rock was sealed with epoxy and silicone to prohibit radial flow within the rock and to restrain heat conduction parallel to the mated rock surfaces.

Additionally, a heat flux sensor was placed in the center beneath the rock adjacent to the heated box, and thermocouples were located on the interfaces between disks radially 1.5 centimeters from the center. The circular aluminum box and rock disks were about 11.5 centimeters in diameter, and the sides and bottom of the aluminum were insulated with fiber board insulation and coated on the outside with RTV silicone. Thus, both the heat flux and temperature gradient normal to the surface of the rock were measured near the center of the fracture.

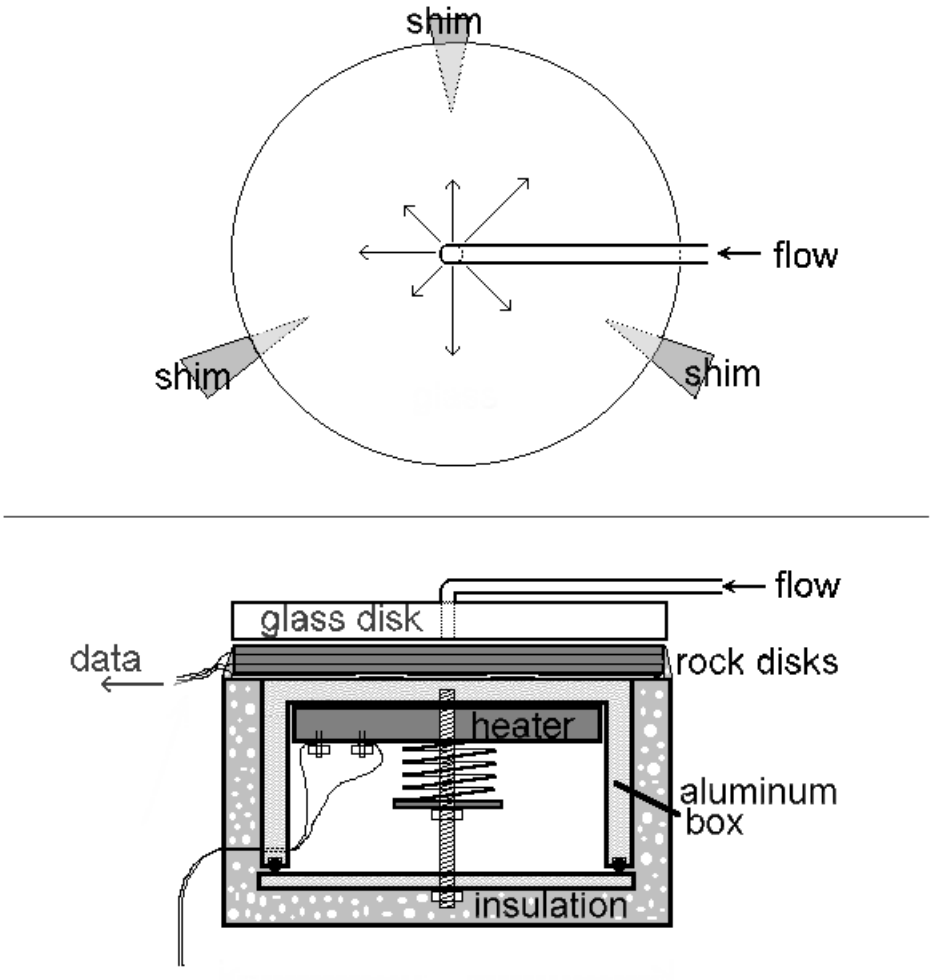

Figure 5.2.1 Heat flux - Temperature gradient measurement experiment. (Steady State)

A uniformly smooth circular fracture was created by compressing a glass disk against three small stainless steel shims which were placed at the outer edge of

the rock. Glass was used to allow observation of the vapor fraction and flow characteristics. Stainless steel shims were used to create an aperture of precise dimension, and the glass disc contained a hole at its center for saturated liquid water to by pumped into the fracture and flow radially outward.

In order to obtain sufficient thermal contact with the rock, a heat sink compound was used between the rock and the aluminum heater box. The rock surface closest to the heater was coated on the heater side with a thin film of high temperature epoxy to prevent the spontaneous imbibition of oil from the heat sink compound from entering the rock. The other surfaces were not treated except that shallow grooves were cut in the rock surfaces for the placement of thermocouples. The top surface of the heater box was engraved to provide for placement of the thermocouples and a heat flux sensor was placed on that surface at the base of the rock. Upon each of the surfaces where temperatures were recorded, three thermocouples were placed 1.5 cm radially out from the center, separated from one another by an angle of 120 degrees. Since the geometry is axisymmetric, two of each set of thermocouples record redundant measurements. Each of the rock disks, from the bottom to the top surface of the rock are, respectively, 3.10 mm, 4.19 mm, and 3.58 mm thick, and a set of three thermocouples were placed at each junction.

5.3 Experimental Procedure

The apparatus was designed to be submersed, however, the following data were collected with the outer edge of the apparatus exposed to the atmosphere. The fracture was oriented horizontally and a small positive displacement pump was used to pump water though a copper coil immersed in boiling water to provide fluid at saturated temperature. The pump was adjusted to supply discrete rates of 15, 30, and 60 ml/min, and the fracture aperture was fixed at either 0.102 mm or 0.889 mm. The average flow velocity was thus varied more than an order of magnitude, and the velocity was further increased as liquid flashed to vapor in the fracture. The average velocity was therefore proportional to both the

volumetric rate and the vapor fraction multiplied by the ratio of the liquid/vapor densities.

Two types of experiments were conducted. The first was a single-phase experiment that investigated the thermal conductivity of the rock by comparing the heat flux measured with ice water injected into the fracture to the steady state temperature gradient. Assuming one-dimensional heat conduction, Fourier's law $q'' = K \Delta T/L$ describes the relationship between the heat flux and the temperature gradient, where the proportionality factor K is the thermal conductivity of the rock. Three temperatures were recorded at ten minute intervals from each thermocouple location while a small amount of power was applied to the heater and ice water was pumped at 30 ml/min with a fracture aperture of 0.102 mm. Ice was also placed on top of the glass disk while temperatures and the heat flux were recorded under these conditions for more than one hour.

The second experiment was a steady state boiling experiment with a much higher maximum temperature and saturated conditions with liquid and vapor flow in the fracture. During this experiment 70 volts and 2 amps were supplied to the heater and were maintained at those levels for the duration of the experiment. Again, temperatures were recorded every ten minutes for many hours while the flow rate and fracture aperture were adjusted and the times of steady state conditions were noted. Unfortunately the heat flux sensor failed during this experiment because the signal from the sensor reached a maximum and would not provide information on heat fluxes above 12022 W/m^2. Therefore, the rock conductivity measured with the single phase experiment was used with the temperature gradient to calculate the heat flux in this experiment.

5.4 Experimental Data and Observations

The arithmetic average temperatures from the data recorded after a steady state had been established are displayed in the plot of Figure 5.4.1, while the average

steady heat flux observed was 11064 W/m^2. A temperature drop of about 130 ^{o}C was measured across the 10.9 mm net thickness of rock. While the overall thermal conductivity of the three rock disks was calculated at 0.92 W / m K, the bottom rock disk which had the epoxy applied to one surface measured 0.53 W / m K, and the middle and top rock disks calculated thermal conductivities of about 1.24 W / m K. While the bottom rock disk displays a thermal conductivity lower than the others, possibly due to its treatment with epoxy, the conductivity of the top two disks appears to be consistent, which is indicated by the uniform slope of the temperature gradient in Figure 5.4.1.

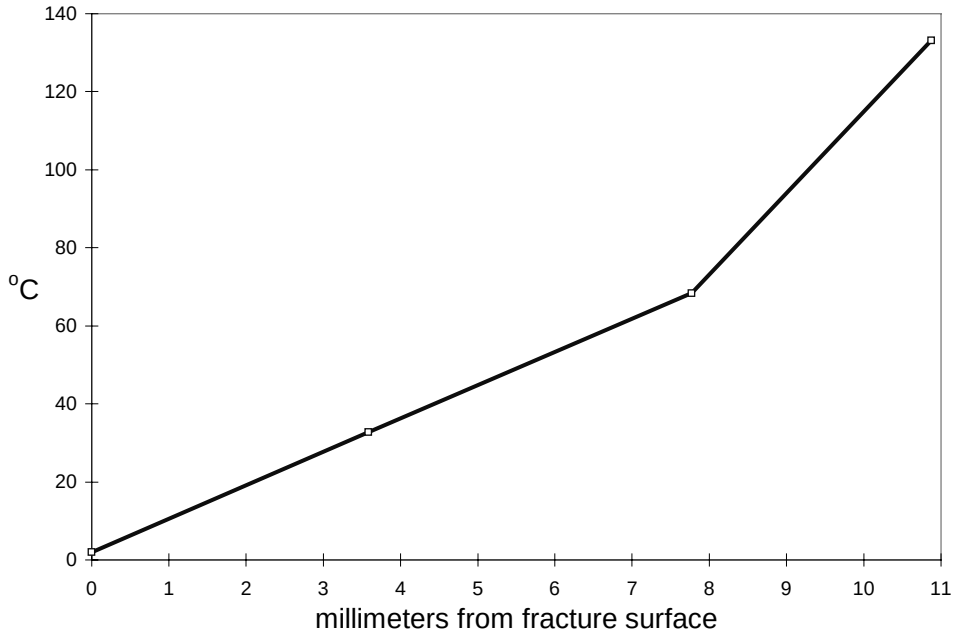

Figure 5.4.1 Steady state temperature distribution with ice water injection.

Data from the high temperature boiling flow experiment are shown in Figure 5.4.2. The arithmetic averages of temperatures from two steady states with water injected at 60 ml/min and 15 ml/min are displayed below in that figure.

As noted earlier, the heat flux sensor read a continuous maximum after the apparatus was heated, so the heat flux was calculated indirectly from the temperature gradient and an assumed thermal conductivity. Assuming the overall thermal conductivity of 0.92 W / m K measured from the ice water

experiment, a calculated heat flux of about 18600 W/m^2 was observed to be practically independent of flow velocity and vapor fraction. Vapor fractions, however, never greatly exceeded about 50%.

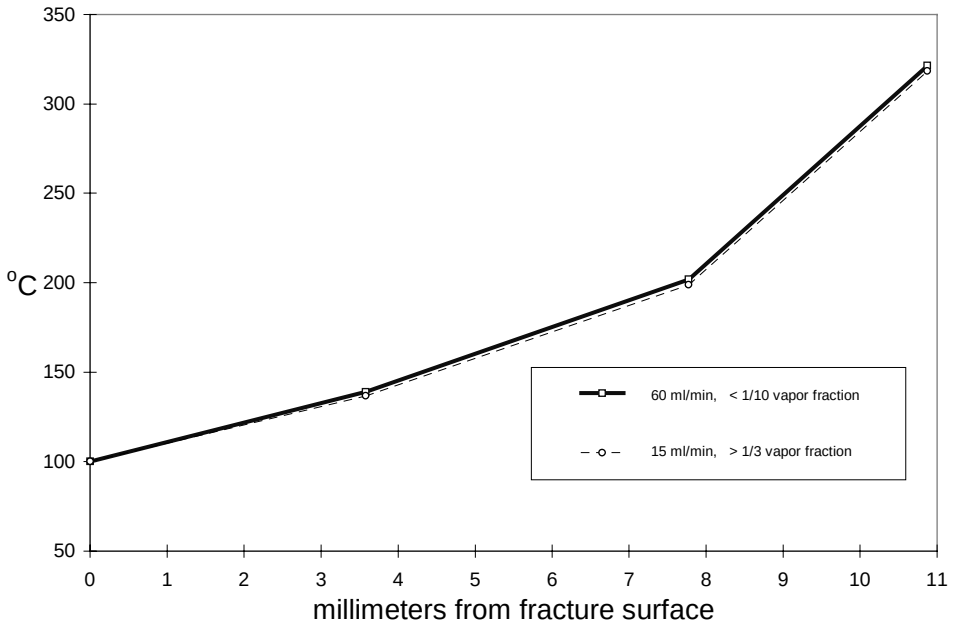

Figure 5.4.2 Steady state temperature distribution during injection / boiling flow.

It was also notable that the two-phase flow could not be described as steady. It was largely axisymmetric, however, a rapid pulsed expansion of vapor in the fracture with a slower return to a greater liquid fraction was observed, especially with the smaller aperture fracture, and at lower flow rates.

5.5 Discussion

When compared with the results of the previous experiments involving transient flow through a narrow glass channel, the data show a significant difference between the heat transfer characteristics of nonporous and porous surfaces. This might be expected, however, even the tiny pores of Geysers core show sufficient permeability for the boiling process to occur just beneath the fracture surface, rather than at the surface, which causes the heat flux to the surface to be only moderately affected by the flow rate and flow regime in the fracture. This

means that the heat advected at the surface of a fracture is not as highly coupled to the flow regime as the boiling heat flux in channels of nonporous materials.

There are uncertainties in the measured temperatures and other derived quantities due to some aspects of how the apparatus was constructed. For example, since the rock disks were cut, ground flat and mated, the pore space and permeability at the junctions of the disks was likely to be much greater than the intrinsic porosity and permeability of the rock. Also, small channels were cut in the rock for the placement of thermocouples, which also created regions of permeability orders of magnitude greater than the natural rock matrix. Since temperatures recorded at symmetric locations the same distance from the fracture surface showed differences of as much as 16 percent, fluid might have unintentionally circulated around the locations of some of the thermocouples and not others.

The thermal conductivity calculated from the temperatures and heat flux in the ice water experiment is notably lower than most measurements of conductivity in Geysers rocks (Walters and Combs, 1991). Since the thermocouples had been checked and calibrated, it would be expedient to check the heat flux sensor by measuring the heat flux and temperature gradient across a well characterized material. Also, thermal conductivity is often a moderate function of temperature, and in a wetted porous rock, would change with the liquid-vapor fraction in the pore space. During the boiling experiment the temperature in part of the rock exceeded 300 ^{o}C. Dependent upon the size of the pores, this may have been sufficient to vaporize much of the liquid in the pores at these high temperatures (Udell 1982). During the high temperature experiment in the apparatus as it was assembled, there may have been thermal contact resistances between the rock disks due to the vaporization of liquid water on those surfaces.

However, if the conductivity of top two rock disks remained consistent, (although it may be a function of temperature), there should have been a nearly linear

temperature gradient through this section of rock to the fracture surface. Since this is not seen in Figure 5.3.2, an extrapolation of the linear trend from the middle rock disk to 100 ^{o}C might indicate the depth within the rock that liquid is circulating, vaporizing, and returning to the flow in the fracture. This idea is illustrated in Figure 5.5.1, where the arrow indicates the location where boiling within the rock alters the temperature gradient to the fracture surface.

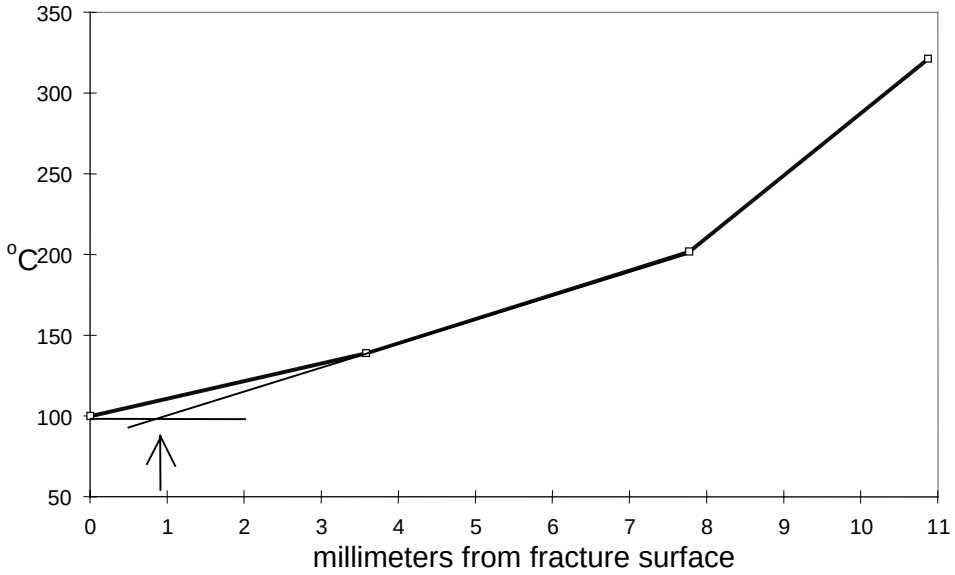

Figure 5.5.1 Extrapolated temperature gradient assuming uniform thermal conductivity.

One conclusion that can be drawn from this concept is that boiling in a fracture is not strictly a surface phenomenon even in very low porosity and low permeability rock, but that the rock porosity and permeability play important roles in reducing the coupling between the heat flux and the liquid/vapor ratio of the flow in the fracture.

Another remarkable observation made during this experiment was that the measured temperatures did not vary significantly when the fracture aperture and pump rates were changed. With volumetric flow rates from 15 to 60 ml/min, with apertures of either 0.102 mm or 0.889 mm, and with vapor fractions that varied

from less than 10 % to more than 50%, the measured temperatures never differed by more than a few degrees Centigrade, well less than the uncertainties associated with those measurements. This is notably unlike the highly coupled flow and boiling in a nonporous walled fracture as seen from the transient experiments.

6 CONCLUSIONS

A comparison of data from the earlier transient experimental apparatus with recent experiments indicates that while heat transfer on nonporous surfaces is strongly coupled to the flow regime, the heat flux to porous rock surfaces with boiling appears to be much less sensitive to the fluid velocity. Therefore, boiling on porous surfaces should be more easily modeled than boiling in nonporous channels. Furthermore, these preliminary experiments show the magnitude of the boiling heat flux to a porous surface is relatively constant, and may depend primarily upon pore thermodynamics. If this is true the boiling convection coefficient may be a relatively simple function of excess temperature and the porosity, permeability, and the size distribution of pores in a particular rock.

Very little research has focused upon the nature of boiling on porous surfaces, and therefore, much more research is needed to understand this phenomenon. Generally, the magnitude of heat advected with boiling is much greater the magnitude of heat advection during single-phase flow. This is positive for establishing steep temperature gradients into unfractured rock and gaining access to greater quantities of thermal energy. This is not positive, however, for numerical modeling because this means that only very finely spaced grids can accurately resolve these temperature gradients.

Multiphase flow in fractures with aperture widths on the order of one millimeter or larger exhibit complicated flow regimes that involve the exchange of momentum between phases. This was demonstrated and videotaped during the transient boiling experiments. Since pressures were not measured, only a qualitative analysis of flow regimes was made. However, observations indicate that a closer study of the interaction of viscous, capillary, inertial and buoyancy forces could help to develop empirical relationships to describe flow velocities and pressure drops in fractured media.

7 REFERENCES

Ambusso, W. J., (1996), Experimental Determination of Steam Water Relative Permeability Relations, MS Report, Dept. Pet. Eng., Stanford University, June 1996.

Bodvarsson, G., (1974), "Geothermal Resource Energetics", Geothermics, vol. 3, no. 3, pp. 83-92, Sept., 1974

Bodvarsson, G. S., and Tsang C. F., (1982), "*Injection and Thermal Breakthrough in Fractured Geothermal Reservoirs*", J. Geophysical Research, vol. 87, no. B2, pp. 1031-1048, Feb. 1982

Boitnott G. N., and Scholtz C. H., (1990), Direct Measurement of the Effective Pressure Law - Deformation of Joints Subject to Pore and Confining Pressures. Journal of Geophysical Research, 95, 19279-19298.

Carslaw, H. W., and Jaeger, J. C., (1959), Conduction of Heat in Solids, 2nd ed. Oxford, Clarendon Press, pg. 396, 1959.

Carey, V. P., *Liquid-Vapor Phase Change Phenomena: An Introduction to the Thermophysics of Vaporization and Condensation Processes in Heat Transfer Equipment.* pp. 508-524, Washington, D. C.: Hemisphere Publishing Corp., 1992.

Chen J., Miller M.A., Sepehrnoori K., (1991). Comparisons of Counter-Current Imbibition Transfer Functions in Dual Porosity Models of Naturally Fractured Reservoirs. In-Situ (1991):115-147.

Chen W.H., Wasserman M.L., Fitzmorris R.E. (1987). A Thermal Simulator for Naturally Fractures Reservoirs. SPE Paper No. 16008, presented at SPE Symposium of Reservoir Simulation, San Antonio, TX, Feb. 1-4, 1987.

Corey A.T., (1954) The Interrelations Between Gas and Oil Relative Permeabilities. Producers Monthly, Vol. 19: pp 38-41.

Council J.R. and Ramey H.J., Jr. (1979) Drainage Relative Permeabilities Obtained from Steam Water Boiling Flow and External Gas Drive Experiments. Geothermal Resources Council Trans. Vol. 3: pp 141-143.

D'Amore, F., Celati, R. and Calore C., (1983), Fluid Geochemistry Applications in Reservoir Engineering (Vapor-Dominated Systems), Proceedings 8th Workshop on Geothermal Reservoir Engineering, Stanford University, Stanford, CA, Dec. 14-16, 1982, 295-308.

DuTeaux R. (1998). Boiling in a Vertical Fracture. Proc. 23rd Workshop on Geothermal Reservoir Engineering, Stanford University, Stanford, CA, Jan 26-28, 1998 (SGP-TR-158)

Faulder D.D., Johnson S.D., Benoit W.R. (1997). Flow and Permeability Structure of the Beowawe, Nevada Hydrothermal System. Proc. 22nd Workshop on Geothermal Reservoir Engineering, Stanford University, Stanford, CA, Jan 27-29, 1997 (SGP-TR-155), 63-71.

Firoozabadi A., Hauge J. (1990). Capillary Pressure in Fractured Porous Media. J Petrol Tech (June 1990):784-791.

Fulcher R.A. Jr., Ertekin T., Stahl C.D. The Effects of Capillary Number and its Constituents on Two-Phase Permeability Curves. SPE Paper No. 12170.

Grant, M. A., Donaldson I.G., and Bixley P.F., Geothermal Reservoir Engineering, pp. 255-256, Academic Press Inc., 1982.

Gringarten A.C., Witherspoon P.A., Ohnishi Y. (1975). Theory of Heat Extraction from Fractured Hot Dry Rock. J Geophysical Res, 90(8):1120-1124.

Gunderson, R.P., (1991), Porosity of Reservoir Graywacke at the Geysers, Geothermal Resources Council, Monograph on The Geysers Geothermal Field, Special Report No. 17, pp. 89-93, 1991.

Harlow, F.H., and Pracht W.E., (1972), A Theoretical Study of Geothermal Energy Extraction, Geophysical Research, 77, 7038, December, 1972.

Hornbrook J., Horne R.N. (1994). The Effects of Adsorption of Injection into Geothermal Reservoirs. Proc. 19th Workshop of Geothermal Reservoir Engineering, Stanford University, Stanford, CA, Jan 18-20, 1994 (SGP-TR-147), 201-207. See also Ph.D. Dissertation, Dept. Pet. Eng. Stanford University, 1994

Horne R.N. (1982). Geothermal Reinjection Experience in Japan. J. Pet. Tech., 34: 495-503

Incropera, F.P., and DeWitt, D.P., *Fundamentals of Heat and Mass Transfer, 3rd Edition*. New York: John Wiley & Sons, 1990.

Kovalev, S.A., Solov'yev S.L., and Ovodkov O.A., (1987), Liquid Boiling on Porous Surfaces, Heat Transfer-Soviet Research, Vol. 19, No. 3, May-June 1987.

Kuo M.C.T., Kruger P., Brigham W.E. (1975), Heat and Mass Transfer in Porous Rock Fragments, Stanford University Geothermal Program Technical Report, No. 10, SGP-TR-10.

Kuo M.C.T., Kruger P., Brigham W.E. (1976). Shape Factor Correlations for Transient Heat Conduction from Irregular-Shaped Rock Fragments to Surrounding Field. Stanford University Geothermal Program Technical Report, No. 16, SGP-TR-16.

Kazemi H., Merrill L.S. (1979). Numerical Simulation of Water Imbibition in Fractured Cores. Soc Petrol Eng J (June 1979):175-182.

Kazemi H., Gilman J.R., Elsharkawy A.M.(1992). Analytical and Numerical Solution of Oil Recovery from Fractured Reservoirs with Empirical Transfer Functions. SPE Res Eng (May 1992):219-227.

Labastie A. (1990). Capillary Continuity between Blocks of a Fractured Reservoir. SPE Paper No. 20515. Presented at the 1990 SPE Annual Technical Conference and Exhibition, New Orleans, LA, Sept 23-26, 1990.

Lung, H., Latsch K., and Rampf H., "*Boiling Heat Transfer to Subcooled Water in Turbulent Annular Flow"* In Hahne, E. and Grigull, U. (eds.) Heat Transfer in Boiling, Hemisphere Publishing, 1997, pp. 220.

Ozdogan, Y., Nolen-Hoeksema R.C., and Nur A., (1994), Pore Pressure Profiles in Fractured and Compliant Rocks, Geophysical Prospecting, Vol. 42, pp. 693-714, 1994.

Pruess K. (1990). Modeling of Geothermal Reservoirs: Fundamental Processes, Computer Simulation, and Field Applications. Geothermics, 19(1):3-15.

Reed, M., (1998), Ultra-low Permeability Core Measurements Taken for The Geysers, Geothermal Technologies, Volume 3, Issue 1, February, 1998.

Robinson, B. A., (1982), Quartz Dissolution and Silica Deposition in Hot Dry Rock Geothermal Systems, Masters Thesis, Massachusetts Institute of Technology, Dept. Of Chem. Eng. Cambridge, MA, 1982.

Rohsenow, W. M., *" A Method of Correlating Heat Transfer Data for Surface Boiling Liquids, Trans,"* ASME, 74, 969-975, 1952.

Tester, J. W., Murphy H. D., Grigsby C. O., Potter R. M., and Robinson B. A., (1989), Fractured Geothermal Reservoir Growth Induced by Heat Extraction, SPE Res. Eng., pp. 97-104, Feb. 1989.

Udell K. (1982). The Thermodynamics of Evaporation and Condensation in Porous Media. SPE Paper 10779. Presented at SPE California Regional Meeting, San Francisco, CA, March 24-26, 1982.

Walters, M. A., and Combs J., (1991), Heat Flow in The Geysers-Clear Lake Geothermal Area of Northern California, U.S.A., Geothermal Resources Council, Monograph on The Geysers Geothermal Field, Special Report No. 17, pp. 43-53.

Warren, J. E., and Root, P. J., (1963), The Behavior of Naturally Fractured Reservoirs, Soc. Pet. Engrs. J., pp. 245-255, Sept., 1963.

Weeler, J. A., (1969), Analytical Calculations for Heat Transfer from Fractures, SPE 2494, Proceedings, SPE of AIME, Mid-Continent Section, Improvd Recovery Symposium, pp. 217-232, April, 1969

Witherspoon P.A., Wang J.C.Y., Iwai K., and Gale J.E. (1980) Validity of the Cubic Law for Fluid Flow in a Deformable Rock Fracture. Water Resources Res., 16, 6, 1016-1024.

Yamagata, K., Kirano F., Nishiwaka K., and Matsuoka H., (1955), Nucleate Boiling of Water on the Horizontal Heating Surface, Mem. Fac. Eng. Kyushu, 15, 98, 1955.